IEEE Access
Multidisciplinary | Rapid Review | Open Access Journal

Received April 28, 2020, accepted May 17, 2020, date of publication May 26, 2020, date of current version June 11, 2020.

Digital Object Identifier 10.1109/ACCESS.2020.2997821

Reduction of Reverse Power Flow Using the Appropriate Size and Installation Position of a BESS for a PV Power Plant

PRAMUK UNAHALEKHAKA AND PANOT SRIPAKARACH
Department of Electrical Engineering, Rajamangala University of Technology Suvarnabhumi, Nonthaburi 11000, Thailand
Corresponding author: Pramuk Unahalekhaka (pramuk.u@rmutsb.ac.th)

ABSTRACT This paper presents an analysis of the appropriate size and installation position of a battery energy storage system (BESS) for reducing reverse power flow (RPF). The system focused on photovoltaic (PV) system power plants. The RPF from the distribution system into the transmission systems impacts the power system due to the increased penetration of the PV system, which produces more power than load. The analysis was divided into three parts: 1) Analysis of the initial load and capacity of the PV power plant; 2) Analysis of the initial load and the load when the capacity of the PV power plant is increased; 3) Analysis of the increased load and capacity of the PV power plant. The stability of the system for each position of the BESS guided the analysis of the reduction of the RPF according to two criteria: reducing the RPF directly and smoothing the distribution load curve. The analysis of the appropriate installation position of the BESS was compared at three positions: 1) at a 115-kV bus; 2) at a 22-kV bus; 3) at a PV power plant. The results of this research showed that the BESS can reduce the RPF and increase the smoothing of the distribution load curve. It can also reduce energy loss and maximum power consumption. However, the appropriate installation position of the BESS was in the PV power plant, because this reduced the energy loss, power fluctuations and electricity production more than installing the BESS at a 115-kV bus or a 22-kV bus.

INDEX TERMS Battery energy storage system (BESS), energy storage system (ESS), photovoltaic system (PV), reverse power flow (RPF), small power producers (SPP), very small power producers (VSPP).

NOMENCLATURE

Cr^{BESS}	Estimated cost of batteries (Baht/kWh)
E^{BESS}	Total BESS energy capacity (MWh)
P^{BESS_Charge}	Charge power (MW)
$P^{BESS\_Discharge}$	Discharge power (MW)
P^{BESS_Rate}	Power rating of BESS (MW)
$PF.$	Power factor
P^{Load}	Load demand (MW)
P^{Load_PV}	Load demand with PV system (MW)
P^{PV}	Power of a PV generator (MW)
P^{Target}	Power target (MW)
Rg^{BESS}	Revenue gained from installation the BESS (million Baht)
S^{TR}	Power rating of the transformer (MVA)
S^{TR}	Power rating of the transformer (MVA)
T^{B}	Lifetime of the battery (years)
V^{Max}	Maximum voltage (V)
V^{min}	Minimum voltage (V)
V^{PCC}	Voltage at the PCC (p.u.)
η^{B}	Efficiency of the battery (%)
η^{TR}	Efficiency of the transformer (%)
Δt	Period of the data change: 15 min.

The associate editor coordinating the review of this manuscript and approving it for publication was Ning Kang.

I. INTRODUCTION

At present, the production of energy from renewable resources in Thailand is increasing because the government has announced several policies to promote the PV system sector. As a result, the number of VSPPs has also increased. For example, a PV system, called a solar farm or PV power plant, can produce electricity for sale only during the daytime, or from approximately 06.00 hrs until 18.30 hrs, which is not enough to control the power flow in 115-kV and 22-kV systems. This results in the PV power plant producing more power than the demand for electricity (load) requires and causes RPF into the transmission system. Therefore, in electric energy storage systems, it is important to control the

power supply, as it has to be appropriate for the load during each period.

Energy storage systems (ESSs) are one of the solutions considered for reducing the number of power plants constructed. They can decrease investment in transmission lines, reduce electricity production and maintain the stability of the power system by, for example, reducing power fluctuations, shifting peak load, and protecting the system from outages [1]. They can be divided into several types: flywheels, capacitors, superconducting magnetic storage systems, compressed air energy storage systems, pumped hydro storage systems, and BESSs [2]–[5].

BESSs have been demonstrated to be critical and effective [6], [7]. For example, in Japan, a BESS was used to reduce fluctuations and to perform constant output control for stabilizing the output of natural energy generators [6], [8] such as wind turbine systems [9]–[11] and PV systems [7], [12]. Additionally, a BESS can perform peak-load shaving in order to save costs by reducing peak grid load [13], [14], balancing peak and off-peak electricity consumption [15], and improving power reliability in the grid, which improves the dispatch ability of renewable energy sources and provides ancillary services to utility grid operations [16], [17].

However, when the power produced by the PV systems in the grid increases, the voltage of the PCC also increases, potentially causing issues for the distribution system [18]–[23]. Therefore, improved voltage regulation methods have been developed to solve the overvoltage issue [24]–[28]. Recent research has demonstrated that BESSs could help to prevent the overvoltage caused by high-penetration PV in distribution systems [23], [29], [30]. Additionally, when the capacity of the PV power plant installed in the distribution system increases, RPF may cause problems [31]–[36] and also affect the power loss [32] both inside and outside of the transmission lines and transformers [33]. Many researchers have proposed solutions to RPF problems, such as using a reverse power relay (RPR), which is simple and reliable for the effective protection against RPF [34]. Proposed cooperative control methods include heat pump water heaters (HPWHs) to reduce RPF, increasing the capacity of storage batteries, and engaging a static var compensator (SVC) by using a supply and demand interface (SDI) [35], [36]. The simulation of a controlled battery charge from solar and wind power generation in 8-20 hrs and a discharge in 0-8 hrs and 20-24 hrs was implemented using MATLAB/Simulink [37]. Particle swarm optimization (PSO) was used to find optimal distributed generation placement (ODGP) for the reduction of RPF [38].

Therefore, ways of increasing the efficiency of BESSs must be analyzed, such as choosing the optimal installation position of a BESS [31], the optimal size of a BESS [13], [29], [30], [39], [40], the optimal size of a BESS for time-of-use rates [39], [41], [42], the optimal grid voltage control [22], the optimal use of existing methods to control the charging and discharging processes [43]–[47], and the BESS type [48].

This paper focuses on the analysis of the appropriate size and installation position of a BESS for the reduction of RPF from the distribution system into transmission systems due to the impact of increased penetration of PV systems, which produce more power than load. The analysis considers three cases.

Case 1: The initial load and capacity of the PV power plant.

Case 2: The initial load with increased capacity of the PV power plant.

Case 3: The increased load and capacity of the PV power plant.

In each of the three cases, the analysis will consider the standard for the voltage at the point of common coupling (PCC), the requirements for installing a PV system in the distribution systems and the load at the highest efficiency of the transformer [49]. The analysis of the appropriate installation position of the BESS will consider three positions:

1) A 115-kV high-side bus in the substation.
2) A 22-kV low-side bus in the substation.
3) A PV power plant in the distribution system.

For each position, the analysis of the reduction of the RPF will consider two criteria: the reduction of the RPF and the smoothing of the distribution load curve. However, as a practical benefit of this paper, there will be an estimated cost analysis of BESSs for the Provincial Electricity Authority (PEA), and the comparison will be performed using the electricity price from the Electricity Generating Authority of Thailand (EGAT) according to the time of use (TOU) rate [50].

II. CASE STUDY OF A POWER SYSTEM NETWORK MODEL

A power system network model in the DigSILENT Power Factory program is selected and modified in this paper to reduce the RPF into the transmission system due to the impact of increased penetration of the PV system for the distribution system of the PEA in Thailand.

A. ABBREVIATIONS AND ACRONYMS

The distribution model includes a fundamental distribution system, which is shown in Figure 1. The model consists of a power transformer (HTM). The HTM has a 115-kV high-side bus and a 22-kV low-side bus. The HTM size is 2 units, and its power rating is 50 MVA. In this type of connection, the primary winding is connected at the delta point and the secondary winding is connected at the star point, with a neutral ground. The distribution system includes two main buses and ten feeders. A PV power plant was installed at each feeder. The distribution model and tools for the network simulation used the Time Sweep function of the DigSILENT Power Factory program to analyze the load profile. Therefore, it can calculate the peak demand for each feeder that follows the standards of the PEA interconnection code [49]

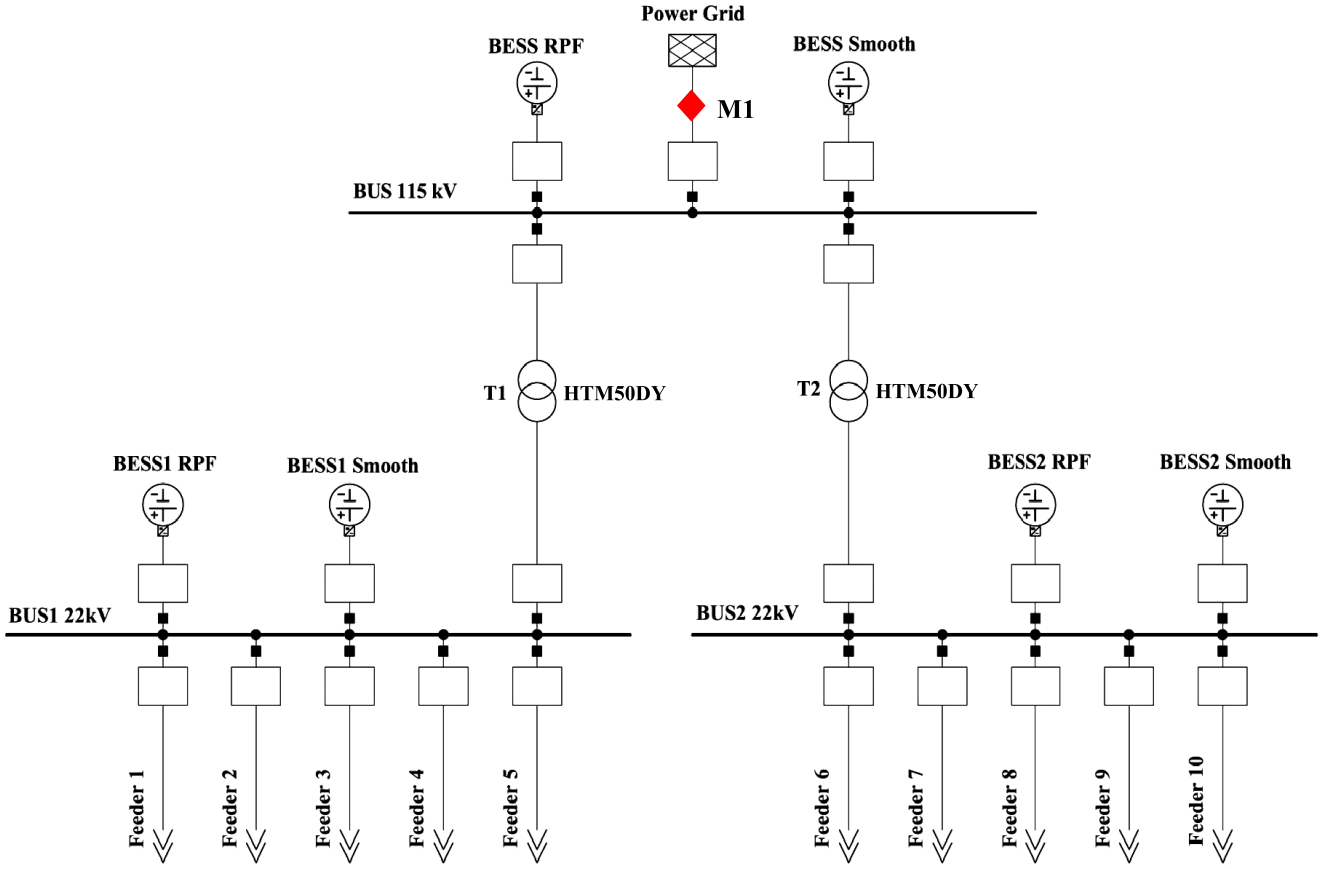

FIGURE 1. Single-line diagram of a radial power system model for the PEA of Thailand.

TABLE 1. Peak demand of the feeders.

Feeder	Peak demand (MW)		
	Case 1	Case 2	Case 3
1	4.92	4.92	7.20
2	-0.37	-0.37	7.20
3	3.27	3.27	7.20
4	5.42	5.42	7.20
5	2.58	2.58	7.20
6	8.49	8.49	8.49
7	4.58	4.58	6.88
8	No Load	No Load	6.88
9	2.29	2.29	6.88
10	4.13	4.13	6.88
Total	**35.31**	**35.31**	**72.01**

given in equation (1).

$$P_{Max}^{Load} = S_{Rate}^{TR} \times \eta_{80\%}^{TR} \times PF. \quad (1)$$

Table 1 shows the calculation of the peak demand for each feeder based on the efficiency of the transformer (80% of the MVA rating). It can be seen that in Cases 1 and 2, there is the same peak demand for the initial load, and the peak demand in Case 3 increases.

Figure 2 shows the load profile without the PV power plant in the three cases; the load profile was measured from the

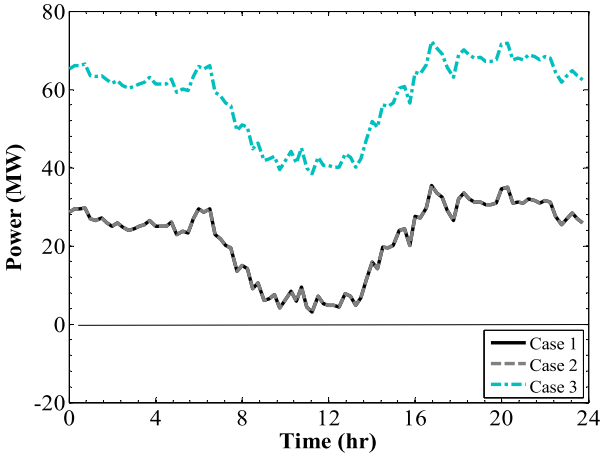

FIGURE 2. Load profile without the PV power plant.

measurement position (M1) in Figure 1. It was found that the total of peak demand is 35.31 MW in Cases 1 and 2 (stable load), and it is 72.01 MW in Case 3 (increasing load).

B. PV POWER PLANT DESCRIPTION

In this section, the capacity of the PV in the three cases is analyzed by considering requirements for installing the PV power plant in the distribution system. Therefore, we calculate the maximum capacity of the PV for each feeder in

TABLE 2. Maximum capacity of PV generation.

At the PCC in the feeder	Maximum capacity of the PV (MW)		
	Case 1	Case 2	Case 3
1	8.00	7.71	6.85
2	8.00	8.00	8.00
3	-	2.75	2.75
4	7.40	7.00	6.79
5	7.40	7.02	6.34
6	7.69	5.96	6.14
7	-	6.39	6.77
8	-	-	8.00
9	2.50	5.67	4.75
10	5.00	8.00	5.00
Total	**45.99**	**58.5**	**61.39**

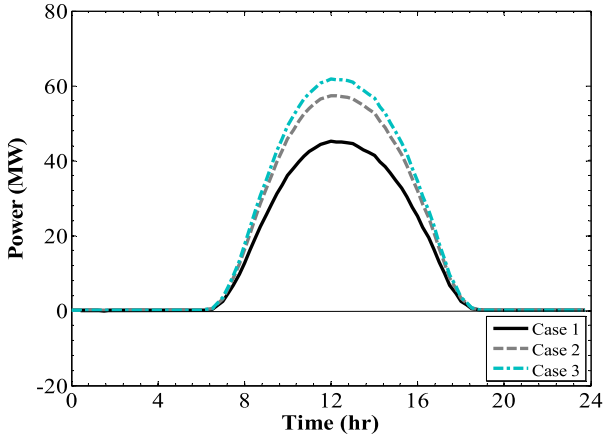

FIGURE 3. PV generation profile for all PV generation.

accordance with the PEA interconnection code [49] with equation (2).

$$P_{Max}^{PV} = S_{Rate}^{TR} \times \eta_{75\%}^{TR} \times PF. \tag{2}$$

Additionally, the voltage standard (±10%) at the PCC must be considered because the protection system (the under- and overvoltage relays) was set based on the voltage standard, which can be calculated by:

$$V_{90\%}^{min} \leq V^{PCC} \leq V_{110\%}^{Max} \tag{3}$$

Table 2 shows the calculated maximum capacity of PV generation according to equation (2) that results in the highest efficiency of the transformer (75% of the MVA rating), but it must not be higher than the voltage standard at the PCC according to equation (3).

The PV generation profile (Figure 3) was measured by using the total PV generation in each case. It was found that the maximum PV generation is 61.39 MW in Case 3 and the minimum PV generation is 45.99 MW in Case 1.

The load profiles with PV generation in Cases 1, 2 and 3 were measured as RPF1, RPF2 and RPF3 respectively, and the measurements were taken from the measurement position (M1) shown in Figure 4. They can be calculated by:

$$P_{y,m,d,t}^{Load\_PV} = P_{y,m,d,t}^{Load} - P_{y,m,d,t}^{PV} \tag{4}$$

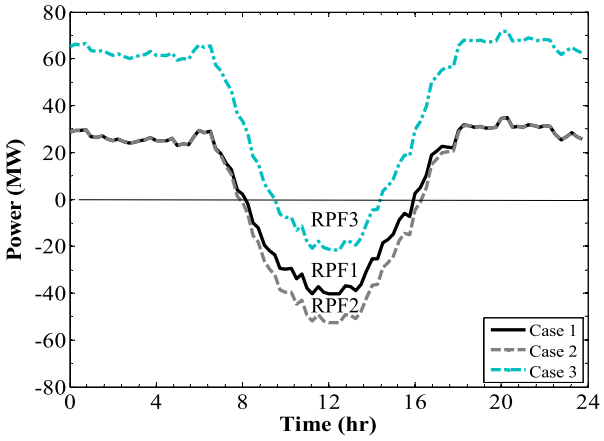

FIGURE 4. Load profile with PV generation.

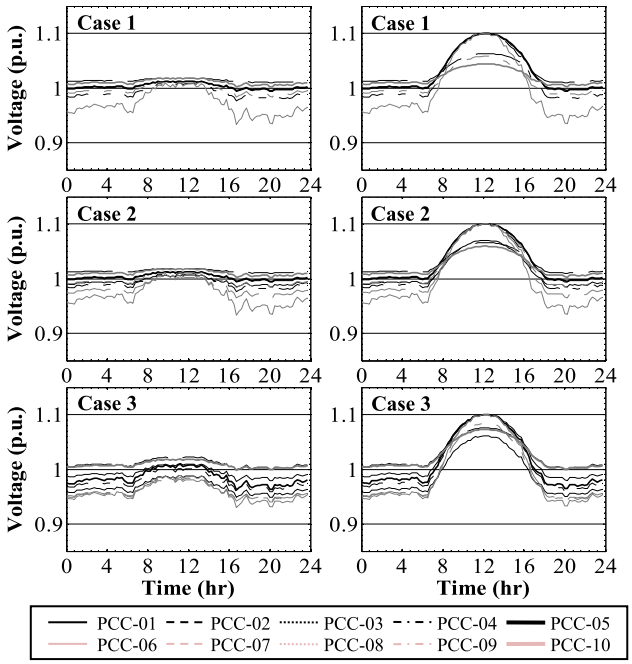

(a) without the PV power plant (b) with the PV power plant

FIGURE 5. Voltage profile at the PCC.

Figure 4 shows that the RPF2 in the transmission system has the highest overall RPF, at 52.73 MW, and RPF3 has the smallest, at 21.47 MW.

The voltage profiles were compared with and without the PV power plant in the distribution system (10 feeders) shown in Figure 5. It was found that when the PV system was installed, the voltage at the PCC increased significantly, in which case the voltage at the PCC was not allowed to go over the voltage standard of the PEA interconnection code shown in equation (3).

The PV power plants were installed at each feeder in the distribution system based on the maximum capacity of PV generation (Table 2) shown in Figure 6.

The results for energy and power were simulated by the time sweep function in the DigSILENT Power Factory

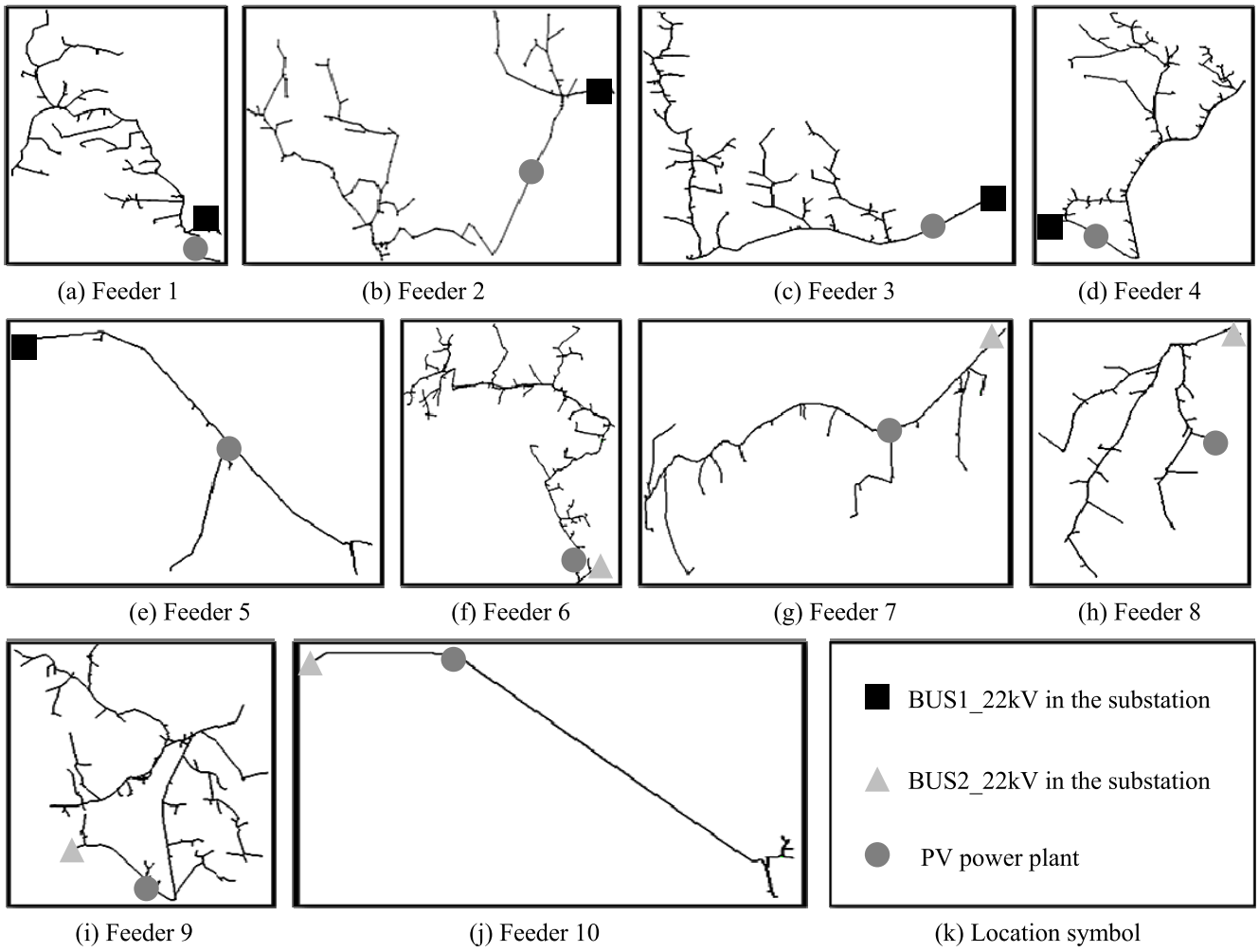

FIGURE 6. Geographical diagram of the distribution system network of the PEA in Thailand. Feeders 1-10 (a-j). Location symbols (k).

TABLE 3. Results for energy and power.

Case	Energy demand (MWh)	Energy RPF (MWh)	Peak load (MW)	Low load (MW)	Total PV (MW)	Energy loss (MWh)
1	408.99	205.84	35.01	-40.47	45.99	33.33
2	399.82	285.28	35.01	-52.73	58.50	33.83
3	1023.74	69.89	71.67	-21.47	61.39	69.93

program in order to analyze the appropriate size and installation position of the BESS, as shown in Table 3.

III. ANALYSIS OF THE APPROPRIATE SIZE AND INSTALLATION LOCATION

This section shows the analysis of the appropriate size and installation location of the BESS in order to reduce the RPF into the transmission systems.

A. ANALYSIS OF THE APPROPRIATE SIZE OF THE BESS

The objectives of the analysis of the appropriate size of the BESS within the power target were determined as follows:

1) The power target for the reduction of the RPF can be calculated by:

$$P_{RPF}^{Target} = 0 \tag{5}$$

2) The power target for the smoothing of the distribution load curve can be calculated by:

$$P_{Smooth}^{Target} = \frac{\sum_{t1}^{t2} (P_{y,m,d,t}^{Load\_PV})}{t2} \tag{6}$$

Examples of the power targets for the reduction of the RPF and the smoothing of the distribution load curve are shown in Figures 7 and 8, respectively.

The charge power was determined in equation (6). The charge powers for the RPF and the smoothing of the distribution load curve are given in equations (7) and (8), respectively.

The discharge power was determined in equation (9). The charge power for the RPF and the smoothing of the distribution load curve are given in equations (10) and (11), respectively.

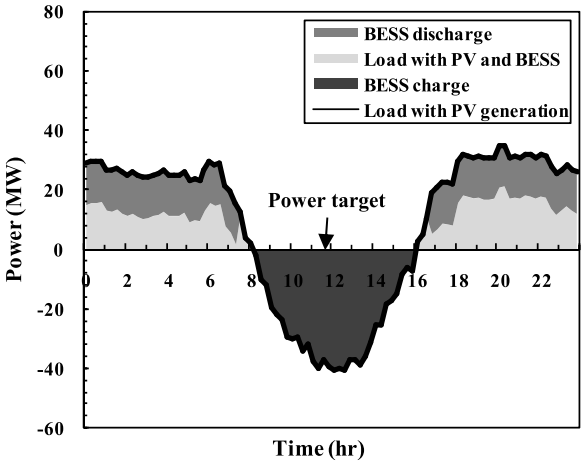

FIGURE 7. Examples of power targets for reduction of the RPF.

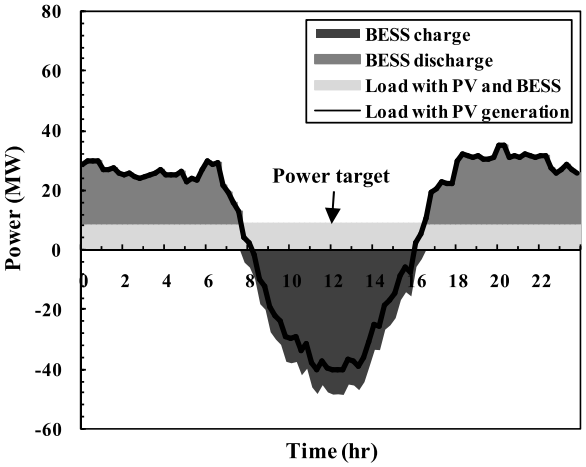

FIGURE 8. Examples of power targets for the smoothing of the distribution load curve.

The charge and discharge power profile of the BESS in all cases was calculated from equations (4)-(11). The reduction of the RPF and the smoothing of the distribution load curve were compared when the BESS was installed at the 115-kV high-side bus in the substation, at the 22-kV low-side bus in the substation, and in the PV power plant in the distribution system. The results show the charge power when the electric power is negative and the discharge power when the electric power is positive, as shown in Figure 9.

$$P^{Load\_PV}_{y,m,d,t} \leq (P^{Target}_{RPF} || P^{Target}_{Smooth}) \tag{7}$$

$$P^{BESS\_Charge}_{y,m,d,t} = P^{Load\_PV}_{y,m,d,t} \tag{8}$$

$$P^{BESS\_Charge}_{y,m,d,t} = P^{Load\_PV}_{y,m,d,t} - P^{Target}_{Smooth} \tag{9}$$

$$P^{Load\_PV}_{y,m,d,t} \geq (P^{Target}_{RPF} || P^{Target}_{Smooth}) \tag{10}$$

$$P^{BESS\_Discharge}_{y,m,d,t} = \frac{\sum_{t1}^{t2} (-P^{BESS\_Charge}_{y,m,d,t})}{T - (t2 - t1)} \tag{11}$$

$$P^{BESS\_Discharge}_{y,m,d,t} = P^{Load\_PV}_{y,m,d,t} - P^{Target}_{Smooth} \tag{12}$$

Therefore, the analysis of the appropriate size of the BESS is based on the determination of 2 characteristics:

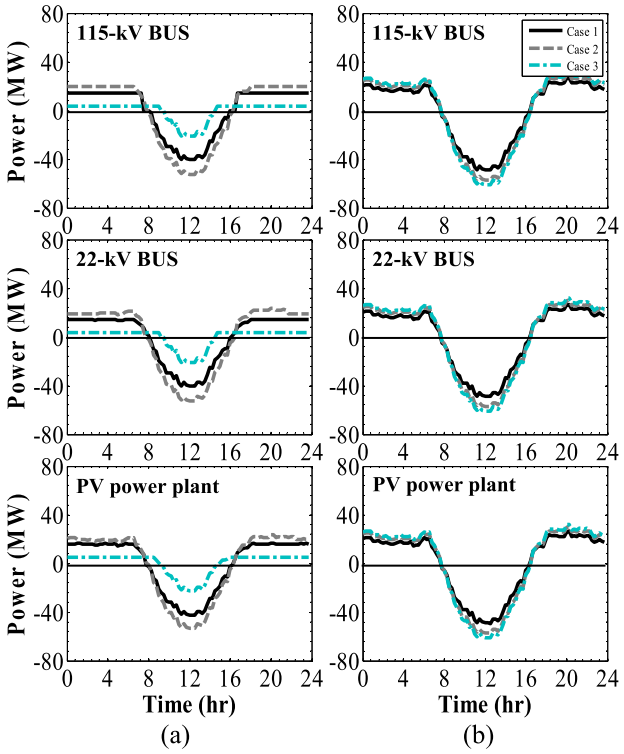

FIGURE 9. Charge and discharge power profiles of the BESS for the reduction of the RPF (a) and the smoothing of the distribution load curve (b).

1) the charging energy of the BESS; 2) the power rating of the BESS. The charging energy of the BESS was calculated as the sum of the charge powers or discharge powers multiplied by the change in time (15 minutes or 0.25 hours). It can be calculated as in equations (12) and (13). Moreover, the power rating of the BESS was determined by the maximum of charge power or discharge as shown in equation (14).

$$E^{BESS} = \sum_{t1}^{t2} \left(P^{BESS\_Charge}_{y,m,d,t} \right) \times \Delta t \tag{13}$$

$$E^{BESS} = \sum_{t1}^{t2} \left(P^{BESS\_Discharge}_{y,m,d,t} \right) \times \Delta t \tag{14}$$

$$P^{BESS\_Rate} \geq (P^{BESS\_Charge}_{MAX} || P^{BESS\_Discharge}_{MAX}) \tag{15}$$

The charging energy and power rating of the BESS for the reduction of the RPF and the smoothing of the distribution load curve are shown in Table 4. Next, we analyze the appropriate installation location of the BESS.

Figure 10 shows the load profile with the BESS in all cases, which was measured from the measurement position (M1) in Figure 1. It was found that the BESS reduced the RPF and increased the smoothing of the distribution load curve. It can also reduce the maximum power consumption rate.

B. APPROPRIATE INSTALLATION LOCATION OF THE BESS

This section shows an analysis of the optimal location of the BESS based on the results for all BESS installation

TABLE 4. Charging energy and power rating of the BESS.

Installation location	Case 1		Case 2		Case 3	
	(MWh)	(MW)	(MWh)	(MW)	(MWh)	(MW)
115-kV BUS for RPF reduction	205.84	40.47	285.28	52.73	69.89	21.47
115-kV BUS for smoothing	276.57	48.94	326.74	57.50	348.80	61.21
22-kV BUS for RPF reduction	210.50	28.11	286.53	29.82	69.90	10.71
22-kV BUS for smoothing	276.65	28.98	326.88	30.18	348.70	30.61
PV power plant for RPF reduction	229.46	7.37	290.89	7.45	81.93	4.05
PV power plant for smoothing	277.21	10.07	327.62	8.16	348.03	7.38

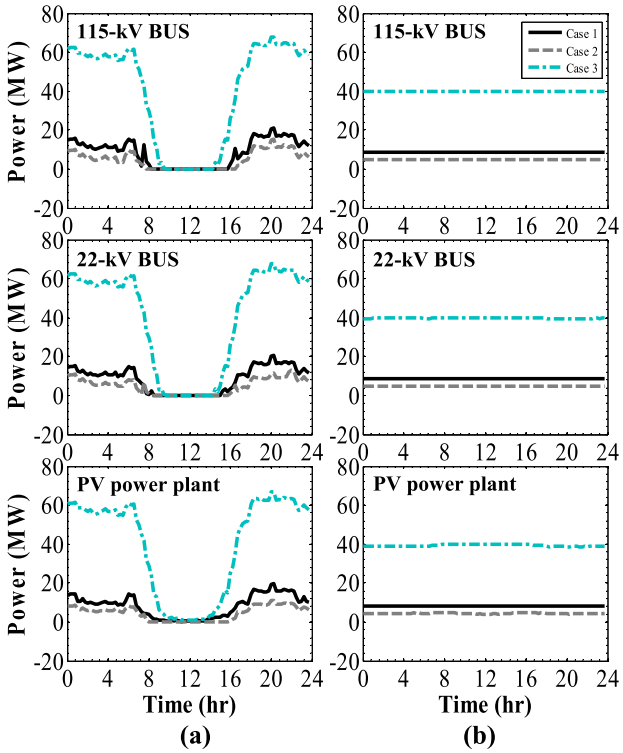

FIGURE 10. Load profile with the BESS for the reduction of the reverse power flow (a) and the smoothing of the distribution load curve (b).

locations that could reduce the energy loss the most, as shown in Table 5 and Figure 11.

Table 5 shows the energy loss in the distribution system before and after the BESS is installed.

Figure 11 shows the power loss profile with the BESS for the reduction of the RPF (a) and the smoothing of the distribution load curve (b). It was found that the energy loss in Case 3 is more than that in Cases 1 and 2, and that installing the BESS in the PV power plant can reduce energy losses more than installing the BESS at the 115-kV BUS or 22-kV BUS in the substation.

Therefore, the best BESS installation location is the PV power plant, since this reduces the energy loss the most, especially by smoothing the distribution load curve.

TABLE 5. Energy loss in the distribution system.

BESS installation locations	Energy loss (MWh)		
	Case 1	Case 2	Case 3
Without BESS	33.71	34.21	70.87
115-kV BUS for RPF reduction	33.66	34.14	70.84
115-kV BUS for smoothing	33.65	34.14	70.78
22-kV BUS for RPF reduction	33.15	33.41	70.44
22-kV BUS for smoothing	33.06	33.37	69.27
PV power plant for RPF reduction	27.40	26.48	67.63
PV power plant for smoothing	26.31	24.97	60.27

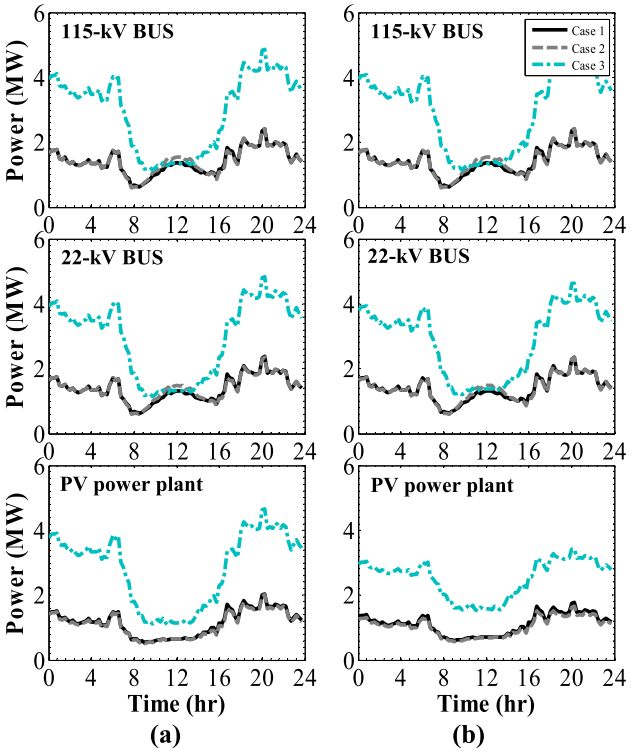

FIGURE 11. Power loss profile with the BESS for the reduction of reverse power flow (a) and the smoothing of the distribution load curve (b).

IV. REASONABLE COST ANALYSIS

This section is an analysis of the estimated cost of the BESS for the investment forecast of BESS installation at the 22-kV BUS in the substation of the PEA. The reason that the estimated cost of the BESS has to be analyzed is that the BESS is very expensive and may not be worth the investment required to install it in the electrical system of Thailand.

Therefore, the analysis of the estimated cost of the BESS can be found from the reduced energy loss by calculating the electricity cost according to the TOU rate in the PEA system [50] shown in Table 6 to find the revenue gained from BESS installation, as shown in Table 7.

Table 6 shows the wholesale electricity charge for the PEA transmission system. The prices are 3.6199 Baht/unit (peak period) and 2.3341 Baht/unit (off-peak period), where peak and off-peak periods are calculated from the average

TABLE 6. Electricity cost based on the time-of-use rate in Thailand for the PEA system.

Voltage system	Electricity cost (THB/kWh)	
	Peak	Off - peak
230 kV	3.3922	3.3922
69 - 115 kV	3.6199	3.6199
11 - 33 kV	4.2243	4.2243

*Unit price: THB (Thai Baht)

TABLE 7. Revenue gained from BESS installation at the PV power plant by smoothing.

Case	Capacity size (MWh)	Power rating (MW)	Reduced energy loss (MWh)	Revenue gained with BESS (million Baht per year)
1	277.21	10.07	7.40	31.32
2	327.62	8.16	9.25	39.28
3	348.03	7.38	10.61	40.20

TABLE 8. Four values of the battery parameter.

Battery technology	Energy efficiency (%)	Lifetime (years)
Lead-acid battery	75 - 85	3 - 12
Lithium-ion battery	90 - 94	5 - 15
Vanadium-based flow battery	70 - 85	5 - 15
Sodium-sulfur battery	75 - 86	5 - 10

numbers of normal days and holidays in 1 year (365 days): 241 normal days, 104 weekend holidays and 20 royal holidays.

Table 7 shows the reduced electrical power loss compared to the revenue gained from the BESS installation in the PV power plant by smoothing. In addition, installing batteries in the PV power plant can help reduce the maximum energy loss. If the size of the BESS increases, the energy loss decreases. Regarding the energy efficiency of the BESS in this research, the analysis is compared across all four types of batteries [51], as shown in Table 8.

The estimated cost analysis of the BESS takes into account the break-even point, the efficiency, and the lifetime of each of the four types of batteries in Table 8, which can be calculated with equation (15).

$$Cr^{BESS} = \frac{Rg^{BESS} \times T^{B} \times \eta^{B}}{E^{BESS}} \tag{16}$$

In this regard, the analysis of the estimated cost of the BESS will be performed based on the performance of the batteries at 5 and 15 years to compare the estimated costs of the four types of batteries, as shown in Table 9.

Table 9 shows the estimated costs of the four types of batteries for BESS installation in the PV power plant for the smoothing of the distribution load curve. It was found

TABLE 9. Estimated cost of batteries for BESS installation at the PV power plant for smoothing.

Case	Battery type	Reasonable cost at lifetime 5 - 15 years (Baht/kWh)
1	Lead-acid	423.73 - 1,440.67
	Lithium-ion	508.47 - 1,593.21
	Vanadium-based flow	395.48 - 1,440.67
	Sodium-sulfur	464.49 - 1,597.86
2	Lead-acid	449.66 - 1,528.83
	Lithium-ion	539.59 - 1,690.71
	Vanadium-based flow	419.68 - 1,528.83
	Sodium-sulfur	493.41 - 1,687.33
3	Lead-acid	433.11 - 1,472.57
	Lithium-ion	519.73 - 1,628.49
	Vanadium-based flow	404.24 - 1,472.57
	Sodium-sulfur	456.64 - 1,570.84

that the estimated cost of the BESS must be lower than 1,440.67 Baht/kWh to break even within 15 years and must be under 395.48 Baht/kWh to break even within 5 years.

V. CONCLUSION

This paper presents an analysis of the appropriate size and installation position of a BESS using the DigSILENT Power Factory program for the reduction of RPF in transmission systems. The analysis results show that a BESS can reduce the RPF and increase the smoothing of the distribution load curve. It can also reduce energy loss and reduce maximum power consumption. The power system is more stable, and revenue is gained from the BESS installation. However, the best installation position of the BESS is in the PV power plant because in this position, the BESS can reduce the energy loss, power fluctuations and electricity production more than if it is installed at a 115-kV high-side bus (21.13% daily reduction in energy loss) or a 22-kV low-side bus (19.09%) in a substation. These results can aid in making the decision to install a BESS for the reduction of RPF in transmission systems.

ACKNOWLEDGMENT

The authors would like to thanks the National Science and Technology Development Agency (NSTDA) and the Energy Policy and Planning Office (EPPO) for supporting this energy storage systems research. In addition, the authors gratefully acknowledge the Provincial Electricity Authority (PEA) for providing the data and support for this work.

REFERENCES

[1] W. A. Omran, M. Kazerani, and M. M. A. Salama, "Investigation of methods for reduction of power fluctuations generated from large grid-connected photovoltaic systems," *IEEE Trans. Energy Convers.*, vol. 26, no. 1, pp. 318–327, Mar. 2011.

[2] M. E. Glavin and W. G. Hurley, "Ultracapacitor/battery hybrid for solar energy storage," in *Proc. 42nd Int. Univ. Power Eng. Conf.*, Sep. 2007, pp. 791–795.

[3] J. M. Carrasco, L. G. Franquelo, J. T. Bialasiewicz, E. Galvan, R. C. PortilloGuisado, M. A. M. Prats, J. I. Leon, and N. Moreno-Alfonso, "Power-electronic systems for the grid integration of renewable energy sources: A survey," *IEEE Trans. Ind. Electron.*, vol. 53, no. 4, pp. 1002–1016, Jun. 2006.

[4] S. S. Choi, K. J. Tseng, D. M. Vilathgamuwa, and T. D. Nguyen, "Energy storage systems in distributed generation schemes," in *Proc. IEEE Power Energy Soc. Gen. Meeting-Convers. Del. Electr. Energy 21st Century*, Jul. 2008, pp. 1–8.

[5] F. Ferdowsi, A. Sadeghi Yazdankhah, and B. Abbasi, "Declining power fluctuation velocity in large PV systems by optimal battery selection," in *Proc. 11th Int. Conf. Environ. Electr. Eng.*, May 2012, pp. 1–6.

[6] H. Li, Y. Iijima, and N. Kawakami, "Development of power conditioning system (PCS) for battery energy storage systems," in *Proc. IEEE ECCE Asia Downunder*, Jun. 2013, pp. 1295–1299.

[7] M. Tamaki, K. Takagi, K. Shimada, N. Kawakami, and Y. Iijima, "Development of PCS for battery system installed in megawatt photovoltaic system," in *Proc. 15th Int. Power Electron. Motion Control Conf. (EPE/PEMC)*, Sep. 2012, pp. 1–4.

[8] N. Kawakami and Y. Iijima, "Overview of battery energy storage systems for stabilization of renewable energy in Japan," in *Proc. Int. Conf. Renew. Energy Res. Appl. (ICRERA)*, Nov. 2012, pp. 1–5.

[9] K. Asanuma, H. Suzaki, and T. Juntsugawa, "Power stabilisation system for wind turbines," *Fuji Jiho*, vol. 81, no. 3, 2008, pp. 203–206.

[10] K. Yoshimoto, T. Nanahara, and G. Koshimizu, "Analysis of data obtained in demonstration test about battery energy storage system to mitigate output fluctuation of wind farm," in *Proc. CIGRE/IEEE PES Joint Symp. Integr. Wide-Scale Renew. Resour. Into Power Del. Syst.*, Jul. 2009, pp. 1–5.

[11] Y. Iijima, Y. Sakanaka, N. Kawakami, M. Fukuhara, K. Ogawa, M. Bando, and T. Matsuda, "Development and field experiences of NAS battery inverter for power stabilization of a 51 MW wind farm," in *Proc. Int. Power Electron. Conf. (ECCE ASIA)*, Jun. 2010, pp. 1837–1841.

[12] M. Akatsuka, R. Hara, H. Kita, T. Ito, Y. Ueda, and Y. Saito, "Estimation of battery capacity for suppression of a PV power plant output fluctuation," in *Proc. 35th IEEE Photovoltaic Spec. Conf.*, Jun. 2010, pp. 541–543.

[13] A. Oudalov, R. Cherkaoui, and A. Beguin, "Sizing and optimal operation of battery energy storage system for peak shaving application," in *Proc. IEEE Lausanne Power Tech*, Jul. 2007, pp. 621–625.

[14] R. T. de Salis, A. Clarke, Z. Wang, J. Moyne, and D. M. Tilbury, "Energy storage control for peak shaving in a single building," in *Proc. IEEE PES Gen. Meeting Conf. Expo.*, Jul. 2014, pp. 1–5.

[15] B.-R. Ke, T.-T. Ku, Y.-L. Ke, C.-Y. Chuang, and H.-Z. Chen, "Sizing the battery energy storage system on a university campus with prediction of load and photovoltaic generation," *IEEE Trans. Ind. Appl.*, vol. 52, no. 2, pp. 1136–1147, Apr. 2016.

[16] B. P. Roberts, "Sodium-sulfur (NaS) batteries for utility energy storage applications," in *Proc. IEEE Power Energy Soc. Gen. Meeting Convers. Del. Electr. Energy 21st Century*, Jul. 2008, pp. 1–2.

[17] K. Mahmud, S. Morsalin, Y. R. Kafle, and G. E. Town, "Improved peak shaving in grid-connected domestic power systems combining photovoltaic generation, battery storage, and V2G-capable electric vehicle," in *Proc. IEEE Int. Conf. Power Syst. Technol. (POWERCON)*, Sep. 2016, pp. 1–4.

[18] R. Tonkoski, D. Turcotte, and T. H. M. El-Fouly, "Impact of high PV penetration on voltage profiles in residential neighborhoods," *IEEE Trans. Sustain. Energy*, vol. 3, no. 3, pp. 518–527, Jul. 2012.

[19] Y. Liu, J. Bebic, B. Kroposki, J. de Bedout, and W. Ren, "Distribution system voltage performance analysis for high-penetration PV," in *Proc. IEEE Energy Conf.*, Nov. 2008, pp. 1–8.

[20] F. Katiraei and J. Aguero, "Solar PV integration challenges," *IEEE Power Energy Mag.*, vol. 9, no. 3, pp. 62–71, May 2011.

[21] Y. Ueda, K. Kurokawa, T. Tanabe, K. Kitamura, and H. Sugihara, "Analysis results of output power loss due to the grid voltage rise in grid-connected photovoltaic power generation systems," *IEEE Trans. Ind. Electron.*, vol. 55, no. 7, pp. 2744–2751, Jul. 2008.

[22] Y. Hayashi, J. Matsuki, S. Kawasaki, S. Hosokawa, and N. Kobayashi, "Optimal grid voltage control in distribution feeder connected with PV systems," in *Proc. IEEE 4th World Conf. Photovoltaic Energy Conf.*, 2006, pp. 2327–2330.

[23] Y. Yang, H. Li, A. Aichhorn, J. Zheng, and M. Greenleaf, "Sizing strategy of distributed battery storage system with high penetration of photovoltaic for voltage regulation and peak load shaving," *IEEE Trans. Smart Grid*, vol. 5, no. 2, pp. 982–991, Mar. 2014.

[24] H. Ravindra, M. Omar Faruque, K. Schoder, M. Steurer, P. Mclaren, and R. Meeker, "Dynamic interactions between distribution network voltage regulators for large and distributed PV plants," in *Proc. PES T&D*, May 2012, pp. 1–8.

[25] X. Liu, A. Aichhorn, L. Liu, and H. Li, "Coordinated control of distributed energy storage system with tap changer transformers for voltage rise mitigation under high photovoltaic penetration," *IEEE Trans. Smart Grid*, vol. 3, no. 2, pp. 897–906, Jun. 2012.

[26] M. Zillmann, R. Yan, and T. K. Saha, "Regulation of distribution network voltage using dispersed battery storage systems: A case study of a rural network," in *Proc. IEEE Power Energy Soc. Gen. Meeting*, Jul. 2011, pp. 1–8.

[27] J. Cappelle, J. Vanalme, S. Vispoel, T. Van Maerhem, B. Verhelst, C. Debruyne, and J. Desmet, "Introducing small storage capacity at residential PV installations to prevent overvoltages," in *Proc. IEEE Int. Conf. Smart Grid Commun. (SmartGridComm)*, Oct. 2011, pp. 534–539.

[28] K. H. Chua, Y. S. Lim, P. Taylor, S. Morris, and J. Wong, "Energy storage system for mitigating voltage unbalance on low-voltage networks with photovoltaic systems," *IEEE Trans. Power Del.*, vol. 27, no. 4, pp. 1783–1790, Oct. 2012.

[29] L. Bitencourt, A. M. Schetinger, B. S. M. C. Borba, D. H. N. Dias, R. S. Maciel, and B. H. Dias, "Maximum PV penetration under voltage constraints considering optimal sizing of BESS on Brazilian secondary distribution network," *IEEE Latin Amer. Trans.*, vol. 14, no. 9, pp. 4063–4069, Sep. 2016.

[30] A. T. Nguyen and S. Chaitusaney, "Optimum schedule and size of BESS in the low voltage network with high penetration of solar rooftops to maintain voltages within acceptable limit," in *Proc. 14th Int. Conf. Electr. Eng./Electron., Comput., Telecommun. Inf. Technol. (ECTI-CON)*, Jun. 2017, pp. 194–197.

[31] M. Hasheminamin, V. G. Agelidis, V. Salehi, R. Teodorescu, and B. Hredzak, "Index-based assessment of voltage rise and reverse power flow phenomena in a distribution feeder under high PV penetration," *IEEE J. Photovolt.*, vol. 5, no. 4, pp. 1158–1168, Jul. 2015.

[32] G. Ramos, D. Celeita, and T. Quintero, "Reverse power flow analyzer (RPFA): A tool to assess the impact of PVs in distribution systems," in *Proc. IEEE Ind. Appl. Soc. Annu. Meeting*, Sep. 2019, pp. 1–6.

[33] E. J. Aladesanmi and D. G. Dorrell, "Investigation and assessment of the impacts of reverse power flow on power system network loading under high penetration of wind energy," in *Proc. Southern Afr. Univ. Power Eng. Conf./Robot. Mechatronics/Pattern Recognit. Assoc. South Afr. (SAUPEC/RobMech/PRASA)*, Jan. 2019, pp. 493–498.

[34] S. Rahman, H. Aburub, M. Moghaddami, and A. I. Sarwat, "Reverse power flow protection in grid connected PV systems," in *Proc. SoutheastCon*, Apr. 2018, pp. 1–5.

[35] H. Hatta, M. Asari, and H. Kobayashi, "Study of energy management for decreasing reverse power flow from photovoltaic power systems," in *Proc. IEEE PES/IAS Conf. Sustain. Alternative Energy (SAE)*, Sep. 2009, pp. 1–5.

[36] H. Hatta, S. Uemura, and H. Kobayashi, "Cooperative control of distribution system with customer equipments to reduce reverse power flow from distributed generation," in *Proc. IEEE PES Gen. Meeting*, Jul. 2010, pp. 1–6.

[37] K. N. Bangash, M. E. A. Farrag, and A. H. Osman, "Manage reverse power flow and fault current level in LV network with high penetration of small scale solar and wind power generation," in *Proc. 53rd Int. Universities Power Eng. Conf. (UPEC)*, Sep. 2018, pp. 1–6.

[38] D. I. Doukas, P. A. Gkaidatzis, A. S. Bouhouras, K. I. Sgouras, and D. P. Labridis, "On reverse power flow modelling in distribution grids," in *Proc. Medit. Conf. Power Gener., Transmiss., Distrib. Energy Convers. (MedPower)*, 2016, pp. 1–6.

[39] A. Meechaka, A. Sangswang, K. Kirtikara, and D. Chenvidhya, "Optimal location and sizing for PV system and battery energy storage system using ABC algorithm considering voltage deviation and time of use rate," in *Proc. 9th Int. Conf. Inf. Technol. Electr. Eng. (ICITEE)*, Oct. 2017, pp. 1–6.

[40] I. Sharma and K. Bhattacharya, "Optimal sizing of battery energy storage systems in unbalanced distribution feeders," in *Proc. 39th Annu. Conf. IEEE Ind. Electron. Soc. (IECON)*, Nov. 2013, pp. 2133–2138.

[41] V. Papadopoulos, T. Delerue, J. Van Ryckeghem, and J. Desmet, "Assessing the impact of load forecasting accuracy on battery dispatching strategies with respect to peak shaving and time-of-use (TOU) applications for industrial consumers," in *Proc. 52nd Int. Univ. Power Eng. Conf. (UPEC)*, Aug. 2017, pp. 1–5.

[42] T.-Y. Lee and N. Chen, "Determination of optimal contract capacities and optimal sizes of battery energy storage systems for time-of-use rates industrial customers," *IEEE Trans. Energy Convers.*, vol. 10, no. 3, pp. 562–568, Sep. 1995.
[43] D. K. Maly and K. S. Kwan, "Optimal battery energy storage system (BESS) charge scheduling with dynamic programming," *IEE Proc. Sci., Meas. Technol.*, vol. 142, pp. 453–458, Nov. 1995.
[44] A. Nagarajan and R. Ayyanar, "Design and strategy for the deployment of energy storage systems in a distribution feeder with penetration of renewable resources," *IEEE Trans. Sustain. Energy*, vol. 6, no. 3, pp. 1085–1092, Jul. 2015.
[45] R. Sebastián, "Application of a battery energy storage for frequency regulation and peak shaving in a wind diesel power system," *IET Gener., Transmiss. Distrib.*, vol. 10, no. 3, pp. 764–770, Feb. 2016.
[46] B. Wang, M. Zarghami, and M. Vaziri, "Energy management and peak-shaving in grid-connected photovoltaic systems integrated with battery storage," in *Proc. North Amer. Power Symp. (NAPS)*, Sep. 2016, pp. 1–5.
[47] Q. Lin, M. Yin, D. Shi, H. Qu, J. Huo, Y. Cheng, G. Li, and J. Li, "Optimal control of battery energy storage system integrated in PV station considering peak shaving," in *Proc. Chin. Autom. Congr. (CAC)*, Oct. 2017, pp. 2750–2754.
[48] B. Jintanasombat and S. Premrudeepreechacharn, "Optimal analysis of battery energy storage for reduction of power fluctuation from PV system in Mae Hong Son province," in *Proc. 5th Int. Youth Conf. Energy (IYCE)*, May 2015, pp. 1–6.
[49] *PEA Regulations Regarding Electrical Network System Connection Requirements*, Thailand, 2016.
[50] *TOU Rates*, Thailand, Nov. 2015.
[51] R. Fu, T. Remo, and R. Margolis, "2018 U.S. Utility-scale photovoltaics plus energy storage system costs benchmark," Nat. Renew. Energy Lab., Tech. Rep., Nov. 2018.

PRAMUK UNAHALEKHAKA was born in Saraburi, Thailand, in December 1973. He received the B.Eng. degree from the Department of Electrical Engineering, Rajamangala Institute of Technology, Thailand, in 1996, and the M.Eng. and D.Eng. degrees from the Department of Electrical Engineering, Kasetsart University, Thailand, in 2002 and 2007, respectively.

He was an Assistant Professor, in 2008. He was also an Associate Professor with the Rajamangala University of Technology Suvarnabhumi, Nonthaburi, Thailand, where he is currently with the Department of Electrical Engineering. His current research interests include renewable energy, power system analysis, and power system protection.

PANOT SRIPAKARACH was born in Bangkok, Thailand, in December 1991. He received the B.Eng. degree from the Department of Electrical Engineering, Thonburi University, Thailand, in 2016, and the M.Eng. degree from the Department of Electrical Engineering, Rajamangala University of Technology Suvarnabhumi, Nonthaburi, Thailand, in 2019.

He is currently with the Department of Electrical Engineering, Thonburi University. His current research interests include renewable energy and power system analysis.